A description of transversely isotropic sound absorbing porous materials by transfer matrices

P. Khurana, L. Boeckx, and W. Lauriks
Laboratorium voor Akoestiek en Thermische Fysica, Katholieke Universiteit Leuven, Celestijnenlaan 200D, B-3001 Heverlee, Belgium

P. Leclaire
Laboratoire de Recherche en Mécanique et Acoustique, Université de Bourgogne, 49 rue Mademoiselle Bourgeois, B.P. 31, 58027 Nevers Cedex, France

O. Dazel and J. F. Allard
Laboratoire d'Acoustique de l'Université du Maine, UMR CNRS 6613, Avenue Olivier Messiaen, F-72085 Le Mans Cedex, France

(Received 2 March 2008; revised 31 October 2008; accepted 3 November 2008)

A description of wave propagation in transversely isotropic porous materials saturated by air with a recent reformulation of the Biot theory is carried out. The description is performed in terms of a transfer matrix method (TMM). The anisotropy is taken into account in the mechanical parameters (elastic constants) and in the acoustical parameters (flow resistivity, tortuosity, and characteristic lengths). As an illustration, the normal surface impedance at normal and oblique incidences of transversely isotropic porous layers is predicted. Comparisons are performed with experimental results. © *2009 Acoustical Society of America.* [DOI: 10.1121/1.3035840]

PACS number(s): 43.55.Ev, 43.20.Gp, 43.20.Jr [SFW] Pages: 915–921

I. INTRODUCTION

A full description of wave propagation through an anisotropic poroelastic material is seldom used for the study of the acoustical behavior of soft highly porous absorbers, which are used for acoustic noise reduction. These materials, such as foams and fibrous materials, may be orthotropic or transversely isotropic, due to their manufacturing process. A more precise optimization of the acoustic performance of these materials, either isolated or as a part of a layered structure, can be achieved by modeling the effects of anisotropy. The theory of wave propagation in anisotropic poroelastic solid was achieved by Biot.[1,2] Since then, many authors, mostly in the field of geophysics, studied the aspects of the wave propagation through anisotropic poroelastic solids and made adaptations on the original formulation of Biot. Carcione[3] analyzed the anisotropic poroelastic media and numerically solved Biot's anisotropic equations. Vashishth and Khurana[4] studied the wave propagation in stratified anisotropic materials taking into account the anisotropy in the elastic constants but neglected the anisotropy in the dynamic permeability. Liu and Liu[5] studied the wave fronts and velocity surfaces of Rayleigh waves in water-saturated orthotropic porous media and indicated the differences with the isotropic and transversely isotropic cases. The wave propagation through highly porous soft absorbers was often studied by using the rigid frame approximation[6–8] and restricted to isotropic media. The use and development of more complete models are mainly limited by the lack of measurement data on the anisotropy of porous sound absorbers. Allard *et al.*[6] measured the effect of the anisotropy in glass wool on the normal surface impedance. They observed deviations in the real part of the surface impedance, which they were able to model using the laws of Delany and Bazley.[9] Several authors investigated the directional differences in material parameters as defined in the Johnson–Allard *equivalent fluid* model. The tortuosity, the viscous characteristic length, and the flow resistivity of open cell foams along the principal axes of the material were measured by Melon *et al.*[10,11] It was shown that there were differences depending on the measurement direction in the mechanical parameters and in the parameters of the rigid frame model. However, there was no description of the acoustical behavior according to the measured material properties. Tarnow[12] proposed an experimental setup allowing the measurement of the elastic constants in a frequency range of 20–160 Hz along the principal axes of symmetry. He gave a complete set of elastic constants for a glass wool considered as a transversely isotropic medium. This allows a modeling of wave propagation in transversely isotropic porous media in terms of a transfer matrix method (TMM) as described in the present work. The anisotropy in mechanical parameters and in the flow resistivity σ, the tortuosity α_∞, and the viscous characteristic length Λ as defined in the Johnson–Allard–Champoux[13–15] model is taken into account. Moreover, a recent formulation[16] of the Biot theory which allows important simplifications in the calculations is used. As an illustration, the TMM is used to predict the surface impedance at normal and oblique incidences of a transversely isotropic soft porous medium of high porosity. Measurement data on the anisotropy factors for the studied material are provided and the influence of these parameters on surface impedance of the material is discussed. Predictions and measurements of the surface impedance are compared.

II. EXPRESSION OF THE SURFACE IMPEDANCE OF A TRANSVERSELY ISOTROPIC POROUS MATERIAL

The surface impedance of a transversely isotropic porous material is predicted from a TMM using the $\{\mathbf{u}^s, \mathbf{u}^t\}$ representation of the Biot model. This representation is based on the use of the displacement vector $\mathbf{u}^s$ of the solid phase and the total displacement $\mathbf{u}^t$ which is defined in what follows. This representation provides a description simpler than the one obtained with both classical representations of the Biot theory. This section is organized as follows: the motion equations are derived, the properties (slowness and polarization) of plane waves are then studied, and the expression of the transfer matrix of a transversely isotropic porous material is obtained. This transfer matrix is then used to obtain the surface impedance of a layer with the axis of symmetry z perpendicular to the faces.

A. $\{\mathbf{u}^s, \mathbf{u}^t\}$ motion equations for a transversely isotropic porous material

Biot[2] extended the isotropic theory for poroelastic materials to the anisotropic case. He took into account the anisotropy in mechanical parameters only but his equations can easily be modified to consider the anisotropy of flow resistivity, tortuosity, and the viscous characteristic length. Let $\mathbf{u}^s$ be the frame displacement and $\mathbf{u}^f$ be the air displacement. Under harmonic excitation at circular frequency ω, the Biot motion equations become

$$\nabla \cdot \sigma^s(\mathbf{u}^s,\mathbf{u}^f) = -\omega^2[\tilde{\rho}_{11}]\mathbf{u}^s - \omega^s[\tilde{\rho}_{12}]\mathbf{u}^f,$$
$$\nabla \cdot \sigma^f(\mathbf{u}^s,\mathbf{u}^f) = -\omega^2[\tilde{\rho}_{12}]\mathbf{u}^s - \omega^2[\tilde{\rho}_{22}]\mathbf{u}^f, \tag{1}$$

where $\mathbf{u}^s$ is the solid phase displacement, $\mathbf{u}^f$ is the fluid phase displacement, $\sigma^s(\mathbf{u}^s,\mathbf{u}^f)$ [respectively, $\sigma^f(\mathbf{u}^s,\mathbf{u}^f)$] is the stress tensor of the solid (respectively, of the fluid) phase, and the $[\tilde{\rho}_{ij}]$ $\{i,j\} \in \{1,2\}$ are diagonal matrices defined by

$$[\tilde{\rho}_{ij}] = \mathrm{diag}(\tilde{\rho}^x_{ij}, \tilde{\rho}^x_{ij}, \tilde{\rho}^z_{ij}). \tag{2}$$

In this equation, the Biot densities $\tilde{\rho}^i_{ij}$, with i replaced by x or z, are given by

$$\tilde{\rho}^i_{12} = \phi\rho_0(1-\tilde{\alpha}^i), \quad \tilde{\rho}^i_{22} = \phi\rho_0 - \tilde{\rho}^i_{12}, \quad \tilde{\rho}^i_{11} = (1-\phi)\rho_s - \tilde{\rho}^i_{12}, \tag{3}$$

where ρ_0 is the density of air, ρ_s is the density of the frame, ϕ is the porosity, and $\tilde{\alpha}^i$ is the dynamic tortuosity in the direction x or in the direction z. In the work by Johnson *et al.*,[13] the dynamic tortuosity is given by

$$\tilde{\alpha}^i_\infty = 1 - \frac{i\phi\sigma^i}{\alpha^i_\infty\rho_0\omega}\sqrt{1 - \frac{4i\alpha^{i2}_\infty\gamma_a\rho_0\omega}{(\sigma^i\Lambda^i\sigma)^2}}, \tag{4}$$

where η_a is the dynamic viscosity of air. With the total displacement formulation,[16] the motion is described in terms of the frame displacement $\mathbf{u}^s$ and the total displacement $\mathbf{u}^t$ given by

$$\mathbf{u}^t = (1-\phi)\mathbf{u}^s + \phi\mathbf{u}^f. \tag{5}$$

The total displacement formulation simplifies the formalism of the Biot theory. This formulation can be extended to the case of transversely isotropic porous media. The strain-stress relations can be written, under the hypothesis that the medium, the frame is made of, is not compressible:

$$-p = \tilde{K}_{\mathrm{eq}}\nabla \cdot \mathbf{u}^t, \quad \sigma^s_{ij} = \hat{\sigma}^s_{ij} - (1-\phi)p\,\delta_{ij}, \tag{6}$$

where p is the interstitial pressure, $\hat{\sigma}^s_{ij}$ is the *in vacuo* stress tensor of the frame which only depends on $\mathbf{u}^s$, and $\tilde{K}_{\mathrm{eq}}$ is the bulk modulus of the fluid modified by the thermal exchanges with the frame,[16] which is given with the Champoux–Allard model by

$$\tilde{K}_{\mathrm{eq}} = (\gamma P_0/\phi)\left\{\gamma - (\gamma-1) \times\left[1 + \frac{8\eta_a}{i\Lambda'\mathrm{Pr}\omega\rho_0}\sqrt{1 + \frac{i\rho_0\omega\mathrm{Pr}\Lambda'^2}{16\eta_a}}\right]\right\}^{-1}. \tag{7}$$

In this equation, P_0 is the atmospheric static pressure, γ is the ratio of the specific heats, Λ' is the thermal characteristic length, and Pr is the Prandtl number. The *in vacuo* stress-strain relations can be written as

$$\begin{aligned}
\hat{\sigma}_{xx} &= (2N+\hat{A})\varepsilon_{xx} + \hat{A}\varepsilon_{yy} + \hat{F}\varepsilon_{zz},\\
\hat{\sigma}_{yy} &= \hat{A}\varepsilon_{xx} + (2N+\hat{A})\varepsilon_{yy} + \hat{F}\varepsilon_{zz},\\
\hat{\sigma}_{zz} &= \hat{F}\varepsilon_{xx} + \hat{F}\varepsilon_{yy} + \hat{C}\varepsilon_{zz},\\
\hat{\sigma}_{yz} &= 2L\varepsilon_{yz}, \quad \hat{\sigma}_{xz} = 2L\varepsilon_{xz}, \quad \hat{\sigma}_{xy} = 2N\varepsilon_{xy}.
\end{aligned} \tag{8}$$

The equations of motion for the $\{\mathbf{u}^s, \mathbf{u}^t\}$ formulation are

$$\nabla \cdot \hat{\sigma}^s = -\omega^2[\tilde{\rho}_s]\mathbf{u}^s - \omega^2[\tilde{\gamma}][\tilde{\rho}_{\mathrm{eq}}]\mathbf{u}^t,$$
$$\tilde{K}_{\mathrm{eq}}\nabla \cdot (\nabla \cdot \mathbf{u}^t[I]) = -\omega^2[\tilde{\gamma}][\tilde{\rho}_{\mathrm{eq}}]\mathbf{u}^s - \omega^2[\tilde{\rho}_{\mathrm{eq}}]\mathbf{u}^t, \tag{9}$$

where $[\tilde{\gamma}]$, $[\tilde{\rho}_{\mathrm{eq}}]$, and $[\tilde{\rho}_s]$ are diagonal matrices given by

$$[\tilde{\gamma}] = \phi\left([\tilde{\rho}_{22}]^{-1}[\tilde{\rho}_{12}] - \frac{1-\phi}{\phi}[I]\right),$$

$$[\tilde{\rho}_{\mathrm{eq}}] = [\tilde{\rho}_{22}]/\phi^2,$$

$$[\tilde{\rho}_s] = [\tilde{\rho}] + [\tilde{\gamma}]^2[\tilde{\rho}_{\mathrm{eq}}].$$

In these equations, the matrix $[I]$ is the identity matrix of size 3 and the matrix $[\tilde{\rho}]=[\tilde{\rho}_{11}]-[\tilde{\rho}_{12}]^2[\tilde{\rho}_{22}]^{-1}$. The equations of motion obtained with the new $\mathbf{u}^s, \mathbf{u}^t$ formulation[16] are simpler than the ones in the previous representations.

B. Plane waves propagating in TIPM

This section is related to poroelastic plane waves.[1] Regardless of the formulation $\{u^s, u^f\}$, $\{u^s, u^t\}$, or $\{u^s, w\}$, for poroelastic medium the solid and fluid displacements follow the same dispersion curve. The methodology of Vashishth and Khurana[4] can then be extended to our formulation.

The acoustic field is created in a transversely isotropic medium by an incident air wave. Without loss of generality, the incidence plane is the xz plane. The angle of incidence is θ. The time dependence is $\exp(i\omega\tau)$. The space dependence for a plane wave can be written as

$$\mathbf{u}^s = \mathbf{a}\exp(-\mathbf{qx}), \quad \mathbf{u}^t = \mathbf{b}\exp(-\mathbf{qx}), \tag{10}$$

where $\mathbf{a}=\{a_x\ a_y\ a_z\}$ and $\mathbf{b}=\{b_x\ b_y\ b_z\}$ are the polarization vectors and $\mathbf{q}=\{q_x=\sin\theta/c_0, q_y=0, q_z\}$ is the slowness vector. The x and y slowness components are those of the incident field. Substituting the expressions for displacement given by Eq. (10) in Eq. (9) provide a homogeneous linear system of six equations which can be split in two sets. One set corresponds to the two y direction equations for the solid displacement and the total displacement and concerns the quasishear horizontal (qSH) waves. The following relations are obtained for these waves:

$$b_y = -\tilde{\gamma}_y a_y, \quad q_z^2 = \frac{1}{L}(\hat{\rho}^x - Nq_x^2). \tag{11}$$

Hence two qSH waves are obtained by taking the square root of q_z^2, a downgoing ($R_{\mathrm{eq}_z}>0$) wave and an upgoing ($R_{\mathrm{eq}_z}>0$) wave. These two waves are not investigated as they are not excited by the incident field. The four remaining equations from Eq. (10) relate the polarizations in the x and the z directions and can be written in the following form:

$$[\mathbf{A}]\{a_x \quad a_z \quad b_x \quad b_z\}^T = \{\mathbf{0}\}, \tag{12}$$

with

$$[\mathbf{A}] = \begin{bmatrix} Lq_x^2 - \tilde{\rho}_s^x + q_x^2\hat{P} & (\hat{F}+L)q_xq_z & -\gamma_x\tilde{\rho}_{\mathrm{eq}}^x & 0 \\ (L+\hat{F})q_xq_z & (\hat{C}q_z^2 + Lq_x^2) - \tilde{\rho}_s^z & 0 & -\gamma_z\tilde{\rho}_{\mathrm{eq}}^z \\ -\gamma_x\tilde{\rho}_{\mathrm{eq}}^x & 0 & -\tilde{\rho}_{\mathrm{eq}}^x + \tilde{K}_{\mathrm{eq}}q_x^2 & \tilde{K}_{\mathrm{eq}}q_xq_z \\ 0 & -\gamma_z\rho_{\mathrm{eq}}^z & \tilde{K}_{\mathrm{eq}}q_x & \tilde{K}_{\mathrm{eq}}q_z^2 - \tilde{\rho}_{\mathrm{eq}}^z \end{bmatrix}. \tag{13}$$

The researched values of q_z correspond to $|\mathbf{A}|=0$ whose expression leads to

$$T_3q_z^6 + T_2q_z^4 + T_1q_z^2 + T_0 = 0, \tag{14}$$

with

$$T_3 = -L\hat{C}\tilde{K}_{\mathrm{eq}}\tilde{\rho}_{\mathrm{eq}}^x, \tag{15}$$

$$T_2 = T_{2,2}q_x^2 + T_{2,0}, \tag{16}$$

$$T_{2,2} = -\tilde{K}_{\mathrm{eq}}[L\hat{C}\tilde{\rho}_{\mathrm{eq}}^z + \tilde{\rho}_{\mathrm{eq}}^x(\hat{P}\hat{C} + L^2 - (\hat{F}+L)^2)], \tag{17}$$

$$T_{2,0} = \tilde{\rho}_{\mathrm{eq}}^x[\tilde{\rho}^x\hat{C}\tilde{K}_{\mathrm{eq}} + L(\hat{C}\tilde{\rho}_{\mathrm{eq}}^z + \tilde{\rho}_{s,z}\tilde{K}_{\mathrm{eq}})], \tag{18}$$

$$T_1 = T_{1,4}q_x^4 + T_{1,2}q_x^2 + T_{1,0}, \tag{19}$$

$$T_{1,4} = -\tilde{K}_{\mathrm{eq}}[L\hat{P}\tilde{\rho}_{\mathrm{eq}}^x + \tilde{\rho}_{\mathrm{eq}}^z(\hat{P}\hat{C} + L^2 - (\hat{F}+L)^2\ ], \tag{20}$$

$$T_{1,2} = \tilde{K}_{\mathrm{eq}}[L(\tilde{\rho}_{\mathrm{eq}}^z\tilde{\rho}^z + \tilde{\rho}_{\mathrm{eq}}^x\tilde{\rho}^x) + \hat{P}\tilde{\rho}_{\mathrm{eq}}^x\tilde{\rho}_s^z + \hat{C}\tilde{\rho}_{\mathrm{eq}}^z\tilde{\rho}_s^x] + \tilde{\rho}_{\mathrm{eq}}^z\tilde{\rho}_{\mathrm{eq}}^x[L^2 + \hat{P}\hat{C} - (F+L)^2 - 2(F+L)\tilde{K}_{\mathrm{eq}}\tilde{\gamma}_x\tilde{\gamma}_z\ , \tag{21}$$

$$T_{1,0} = -\tilde{\rho}_{\mathrm{eq}}^x[L\tilde{\rho}_{\mathrm{eq}}^x\tilde{\rho}^z + \hat{C}\tilde{\rho}_{\mathrm{eq}}^z\tilde{\rho}_x + \tilde{K}_{\mathrm{eq}}\tilde{\rho}^x\tilde{\rho}_s^z], \tag{22}$$

$$T_0 = T_{0,6}q_x^6 + T_{0,4}q_x^4 + T_{0,2}q_x^2 + T_{0,0}, \tag{23}$$

$$T_{0,6} = -\tilde{\rho}_{\mathrm{eq}}^zL\hat{P}\tilde{K}_{\mathrm{eq}}, \tag{24}$$

$$T_{0,4} = \tilde{\rho}_{\mathrm{eq}}^z[L(\tilde{K}_{\mathrm{eq}}\tilde{\rho}_s^x + \hat{P}\tilde{\rho}_{\mathrm{eq}}^x) + \tilde{\rho}^x\hat{P}\tilde{K}_{\mathrm{eq}}], \tag{25}$$

$$T_{0,2} = -\tilde{\rho}_{\mathrm{eq}}^z[L\tilde{\rho}^x\tilde{\rho}_{\mathrm{eq}}^x + \tilde{\rho}_z(\tilde{K}_{\mathrm{eq}}\tilde{\rho}_s^x + \hat{P}\tilde{\rho}_{\mathrm{eq}}^x)], \tag{26}$$

$$T_{0,0} = \tilde{\rho}_{\mathrm{eq}}^z\tilde{\rho}^z\tilde{\rho}^x\tilde{\rho}_{\mathrm{eq}}^x. \tag{27}$$

There are no odd terms in this cubic polynomial in q_z^2. Each root provides two square roots. These can be numbered with the index $k=1,2,3$ for the downgoing waves and $k+3$ for the upgoing waves. For each q_z, the polarization of the wave can be normalized so that $b_z=1$

$$\{a_x, a_z, b_x, b_z\} \propto \{\mu_{x,s}, \mu_{z,s}, \mu_{x,t}, 1\}. \tag{28}$$

This normalization does not allow a null z total displacement component, but there is no restriction to use it in our context. The coefficients μ can be written as

$$\mu_{x,t} = \frac{-(\gamma_zq_{c,z}^2q_xq_z)[(P_0q_x^2) + L_0q_z^2 - q_{s,x}^2] - (\gamma_xq_{c,x}^2q_xq_z)(q_z^2 - q_{\mathrm{eq},z}^2)}{\gamma_zq_{c,z}^2[(P_0q_x^2 + L_0q_z^2 - q_{s,x}^2)(q_x^2 - q_{\mathrm{eq},x}^2) - \gamma_xq_{c,x}^2q_{e,x}^2] + \gamma_zq_{c,z}^2q_z^2q_x^2}, \tag{29}$$

where $P_0=\hat{P}/(L+\hat{F})$ and $L_0=L/(L+\hat{F})$,

$$\mu_{z,s}=\frac{\widetilde{K}_{\text{eq}}[(q_z^2-q_{\text{eq},z}^2)+q_zq_x\mu_{x,t}]}{(L+\hat{F})\widetilde{\gamma}_z q_{c,z}^2}, \tag{30}$$

$$\mu_{x,s}=\frac{\widetilde{K}_{\text{eq}}(q_zq_x+(q_x^2-q_{\text{eq},x}^2)\mu_{x,t})}{(L+\hat{F})\widetilde{\gamma}_z q_{c,z}^2}, \tag{31}$$

with the slownesses of the material

$$q_{\text{eq},i}=\sqrt{\frac{\widetilde{\rho}_{\text{eq}}^i}{\widetilde{K}_{\text{eq}}}},\quad q_{c,i}=\sqrt{\frac{\widetilde{\rho}_{\text{eq}}^i}{L+\hat{F}}},\quad q_{s,i}=\sqrt{\frac{\widetilde{\rho}_s^i}{L+\hat{F}}}. \tag{32}$$

The following parity/imparity relations are used for the up-going waves:

$$\mu_{x,t}(k+3)=-\mu_{x,t}(k),\quad \mu_{z,s}(k+3)=\mu_{z,s}(k),$$
$$\mu_{z,s}(k+3)=-\mu_{x,s}(k). \tag{33}$$

C. Expression of the transfer matrix of a transversely isotropic layer in the $\{\mathbf{u}^s,\mathbf{u}^t\}$ formulation

A transfer matrix connecting state vectors describing the mechanical field at each plane boundary of an anisotropic elastic medium was used by Brekhovskikh.[17] In this case, the mechanical field can be described by two waves which propagate toward increasing z and two waves which propagate toward decreasing z. The field in the medium is completely described if four amplitudes of these waves or for independent quantities describing the field are known. In this case, a state vector with four components is used. The first use of a transfer matrix for isotropic porous media was performed by Depollier.[18] Three kinds of waves, in context of the Biot theory, can propagate in an isotropic porous medium and the state vector has six components. The number of components is also 6 for a trans (TIPM)] if only the waves polarized in the meridian plane are present.

The transfer matrix provides a relation between state vectors of the medium at two different z. The state vector at a generic position $z=l$ is defined by

$$V(l)=[\dot{u}_z^s(l)\quad \dot{u}_x^s(l)\quad \dot{u}_z^t(l)\quad p(l)\quad \hat{\sigma}_{xz}(l)\quad \hat{\sigma}_{zz}(l)]^t. \tag{34}$$

This state vector is conserved at the interface between two porous media and it allows a simple coupling with air.[16] The transfer matrix is obtained with the method described in Refs. 4, 15, 19, and 20. Each component of the state vector can be expressed as a sum of the contributions of the six waves. For example, the z solid phase velocity components at $z=0$ and at $z=H$ are linked to the amplitudes f_k of the waves by

$$\dot{u}_z^s(0)=\sum_{k=1}^{6} r_1(k)f_k,\quad \dot{u}_z^s(H)=\sum_{k=1}^{6} r_1(k)e_kf_k, \tag{35}$$

where

$$r_1(k)=i\omega\mu_{z,s}(k),\quad e_k=\exp(i\omega q_z(k)H),$$
$$k=1,2,3,\quad e_{k+3}=\frac{1}{e_k}, \tag{36}$$

and f_k denotes the amplitude of the waves. Similar equations can be obtained from the five remaining components of the state vector which involve the functions r_i, $i=2,3,4,5,6$:

$$r_2(k)=i\omega\mu_{x,s}(k),\quad r_3(k)=i\omega, \tag{37}$$

$$r_4(k)=\lambda_p(k),\quad r_5(k)=\lambda_x(k),\quad r_6(k)=\lambda_z(k), \tag{38}$$

where the λ are given by

$$\lambda_x(k)=-iL\omega[q_z(k)\mu_{x,s}+q_x\mu_{z,s}],\quad \lambda_x(k+3)=\lambda_x(k), \tag{39}$$

$$\lambda_z(k)=-i\omega[\hat{F}q_x\mu_{x,s}+\hat{C}q_z(k)\mu_{z,s}],\quad \lambda_z(k+3)=-\lambda_z(k), \tag{40}$$

$$\lambda_p(k)=i\omega\hat{K}_{\text{eq}}[q_x\mu_{x,t}+q_z(k)],\quad \lambda_p(k+3)=-\lambda_p(k). \tag{41}$$

The transfer matrix $[\mathbf{T}]$ can be defined by

$$\mathbf{V}(H)=[\mathbf{T}]\mathbf{V}(0). \tag{42}$$

The matrix elements are given by

$$T_{ij}=\sum_{k=1}^{3}\left(e_k+\frac{(-1)^{i+j}}{e_k}\right)r_i(k)c_j(k), \tag{43}$$

where

$$c_1(k)=\frac{\lambda_x(k^+)-\lambda_x(k^{++})}{i\omega\Delta_2}, \tag{44}$$

$$c_2(k)=\frac{\lambda_p(k^+)\lambda_z(k^{++})-\lambda_p(k^{++})\lambda_z(k^+)}{i\omega\Delta/\Delta_1}, \tag{45}$$

$$c_3(k)=\frac{\mu_{z,s}(k^+)\lambda_x(k^{++})-\mu_{z,s}(k^{++})\lambda_x(k^+)}{i\omega\Delta_2}, \tag{46}$$

$$c_4(k)=\frac{\mu_{x,s}(k^{++})\lambda_z(k^+)-\mu_{x,s}(k^+)\lambda_z(k^{++})}{\Delta/\Delta_1}, \tag{47}$$

$$c_5(k)=\frac{\mu_{z,s}(k^{++})-\mu_{z,s}(k^+)}{\Delta_2}, \tag{48}$$

$$c_6(k)=\frac{\lambda_p(k^{++})\mu_{x,s}(k^+)-\lambda_p(k^+)\mu_{x,s}(k^{++})}{\Delta/\Delta_1}, \tag{49}$$

$$\Delta_1=4\frac{\sum_{k=1}^{3}\mu_{z,s}(k)(\lambda_x(k^+)-\lambda_x(k^{++}))}{e_1e_2e_3}, \tag{50}$$

$$\Delta_2=2e_1e_2e_3\sum_{k=1}^{3}\mu_{x,s}(k)(\lambda_p(k^+)-\lambda_p(k^{++})), \tag{51}$$

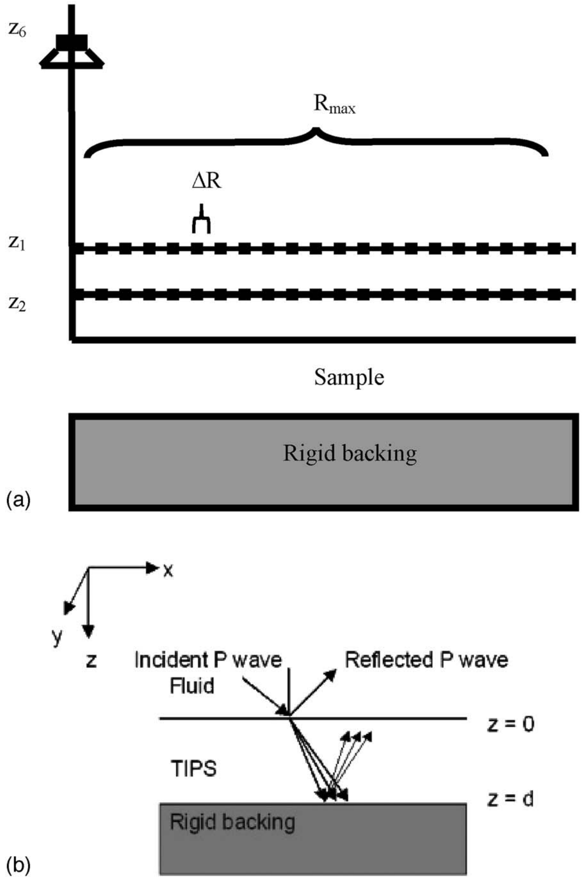

FIG. 1. (a) Experimental setup and indication of the respective geometrical parameters. (b) Geometry of model.

$$\Delta = -8\left[\sum_{k=1}^{3} \lambda_p(k^+)(\mu_{x,s}(k^+)\lambda_z(k^{++}) - \mu_{x,s}(k^{++})\lambda_z(k^+))\right] \times \left[\sum_{k=1}^{3} \lambda_x(k)(\mu_{z,s}(k^{++}) - \mu_{z,s}(k^+))\right]. \quad (52)$$

In all the preceding expressions, the $+$ (respectively, $++$) superscript corresponds to a first (respectively, second) following index in circular permutation of the {1,2,3} set (for instance, $2^+=3$, $2^{++}=1$). The new expressions of the $T_{i,j}$ are simpler than the previous expressions obtained in Refs. 4, 15, and 20. They can be more easily implemented in scientific programs.

D. Expression of the surface impedance

The porous layer of thickness H is bonded onto a rigid impervious backing (see Fig. 1). At $z=H$ on the rigid backing, the displacement components are equal to 0

$$\mathbf{V}(H) = [0 \quad 0 \quad 0 \quad p(H) \quad \hat{\sigma}_{xz}(H) \quad \hat{\sigma}_{zz}(H)]^t. \quad (53)$$

At $z=0$, the following conditions must be satisfied:

$$\mathbf{V}(0) = [\dot{u}_z^s(0) \quad \dot{u}_x^s(0) \quad \dot{u}_z^t(0) = v_z^{\mathrm{air}} \quad p(0) = p^{\mathrm{air}} \quad 0 \quad 0]^t, \quad (54)$$

where p^{air} and v^{air} are the pressure and the normal velocity in the free air at the interface with the porous material. The surface impedance is defined by $Z=p^{\mathrm{air}}/v_z^{\mathrm{air}}$ and Zv^{air} can be substituted for p^{air} in the preceding equations. The three displacement components at $z=H$ can be obtained from the components of $\mathbf{V}(0)$, leading to the following system of three equations.

TABLE I. Acoustical and mechanical parameters of the porous material.

Thickness	H	cm	6
Frame density	ρ_s	kg/m^3	60
Porosity	ϕ		0.99
Flow resistivity (perpendicular)	σ^z	N m^{-4} s	17 000
Flow resistivity (parallel)	$\sigma^{x'y}$	N m^{-4} s	5000
Viscous dimension (perpendicular)	Λ^z	μm	140
Viscous dimension (parallel)	$\Lambda^{x,y}$	μm	126
Thermal dimension	Λ'	μm	150
Tortuosity (perpendicular)	α_∞^z		1.01
Tortuosity (parallel)	$\alpha_\infty^{x,y}$		1.01
Shear modulus (perpendicular)	L	kPa	50+i7
Shear modulus (parallel)	N	kPa	120+i22

$$T_{11}\dot{u}_z^s + T_{12}\dot{u}_x^s + (T_{13} + ZT_{14})v_z^{\mathrm{air}} = 0, \quad (55)$$

$$T_{21}\dot{u}_z^s + T_{22}\dot{u}_z^s + (T_{23} + ZT_{24})v_z^{\mathrm{air}} = 0, \quad (56)$$

$$T_{31}\dot{u}_z^s + T_{32}\dot{u}_x^s + (T_{33} + ZT_{34})v_z^{\mathrm{air}} = 0. \quad (57)$$

The determinant of the system must be equal to 0 and Z is given by

$$Z = -\begin{vmatrix} T_{11} & T_{12} & T_{13} \\ T_{21} & T_{22} & T_{23} \\ T_{31} & T_{32} & T_{33} \end{vmatrix} \Bigg/ \begin{vmatrix} T_{11} & T_{12} & T_{14} \\ T_{21} & T_{22} & T_{24} \\ T_{31} & T_{32} & T_{34} \end{vmatrix}. \quad (58)$$

III. PREDICTIONS AND MEASUREMENT OF THE SURFACE IMPEDANCE

A. Acoustical and mechanical parameters

The material is a layer of glass wool of thickness 6 cm. The layer is transversely isotropic with the symmetry axis, the z axis in Fig. 1, perpendicular to the surface. The acoustic parameters and rigidity coefficients that are given in Table I were all measured. Standard methods exist for measuring the flow resistivity and porosity. Tortuosity, viscous characteristic, and thermal characteristic length were measured using ultrasonic transmission methods (see Refs. 10, 11, and 21). These methods were originally proposed for isotropic porous materials. For the fibrous material under investigation, cylindrical samples were cut according to the principal axes. The acoustical parameters were determined for these cylindrical samples, on which also impedance tube measurements were performed. It was verified that the results of the impedance tube could be modeled by a numerically calculated absorption coefficient based on the individually measured acoustical parameters given in Table I. The shear modulus L in a plane perpendicular to the surface and the shear modulus N in a plane parallel to the surface have been measured at low frequencies using a similar technique as the one developed by Etchessahar *et al.*[20] The Poisson ratios are negligible for glass wools[12] and the rigidity coefficients $\hat{F}$ and $\hat{A}$ are equal

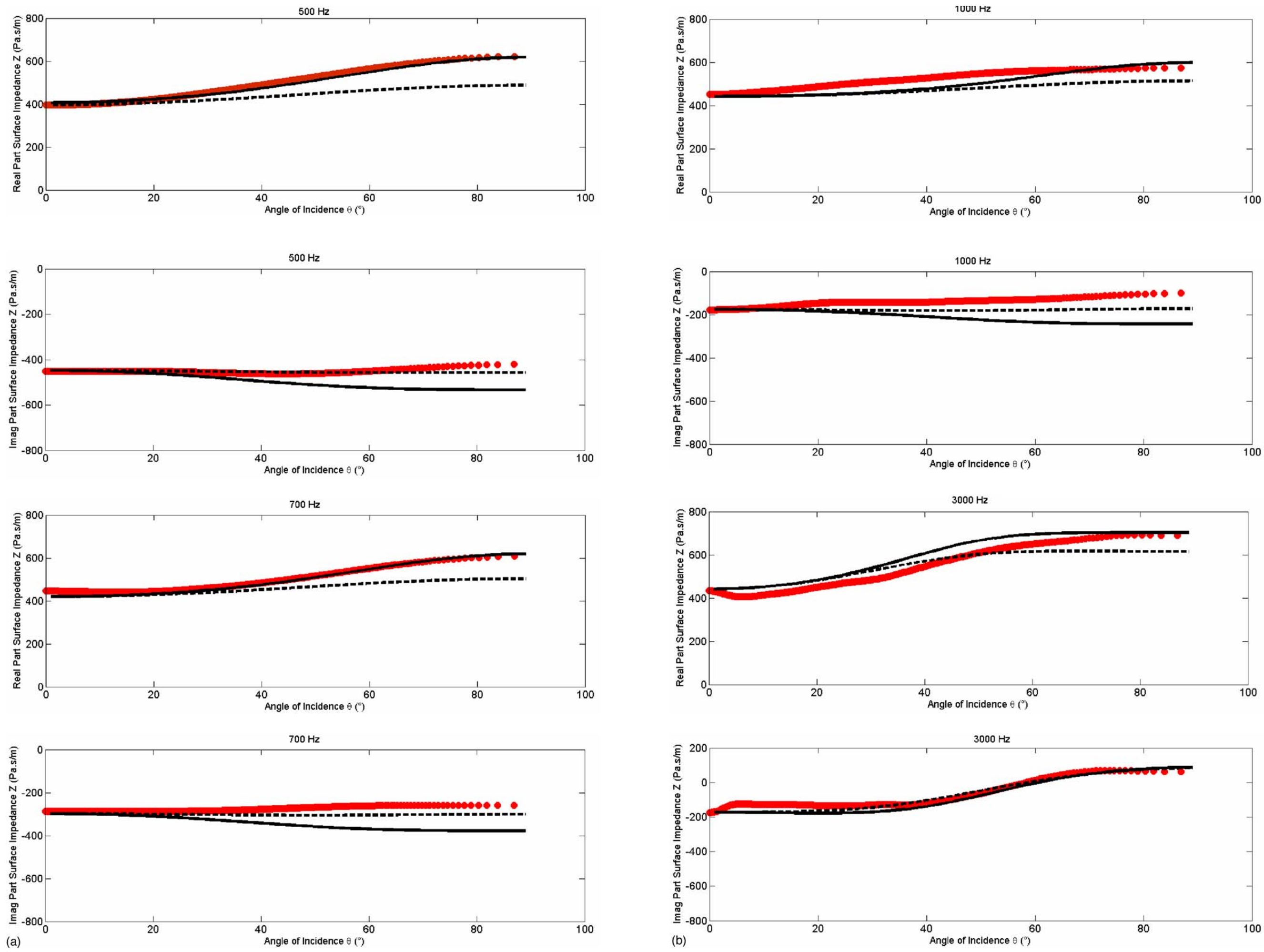

FIG. 2. (Color online) (a) Real and imaginary parts of the surface impedance for 0.5 kHz [(i) and (ii)] and 0.7 kHz [(iii) and (iv)] as a function of angle of incidence. Measurements are indicated by circles, dashed lines indicate calculated impedances for the isotropic case, and solid lines indicate the calculated impedances taking the anisotropy into account. (b) Real and imaginary parts of the surface impedance for 1 kHz [(i) and (ii)] and 3 kHz [(iii) and (iv)] as a function of angle of incidence. Measurements are indicated by circles, dashed lines indicate calculated impedances for the isotropic case, and solid lines indicate the calculated impedances taking the anisotropy into account.

to zero. Due to the large loss angle of the coefficients and the fact that the frame density is much larger than the air density, the frame displacement induced by a pressure field in the free air is very small compared to the displacement of the saturating air. The surface impedance will not strongly dependent on the rigidity coefficients, and $\hat{C}$ is arbitrarily set equal to $2L$, like if the meridian plane were an isotropic plane. A sensitivity analysis also showed that, for the fibrous material under investigation, the calculated surface impedance was only minor dependent on the measured values of tortuosity, viscous, and thermal characteristic lengths. The ratio of flow resistivities proved to have the largest influence on the calculated surface impedances of fibrous materials, which was also pointed out by Ref. 6.

B. Surface impedance measurement

The measurement of the surface impedance was performed by using the near-field holographic method introduced by Tamura *et al.*[22,23] The method initially relied on the decomposition of the wave field into its plane wave components by means of spatial Fourier transformation. In the present version of the Tamura method, the acoustic field created by the source is axisymmetric and the Fourier transform is replaced by the Hankel transform. A sketch of the experimental setup is represented in Fig. 1. The fibrous material is glued to a rigid backing and an unbaffled loudspeaker which is a dipole source with a good approximation that is placed at $z_s = 10$ cm above the sample. The sound pressure is measured at $z_1 = 10$ mm and $z_2 = 16$ mm. The pressure is measured at radial distances of the source ranging from $R = 0$ m up to $R_{\max} = 1.4$ m; the interval ΔR between two measurements is equal to 2 mm. The input signal is a sine sweep ranging from 100 Hz to 7 kHz. At each measurement, the transfer function between the measured and the input signal is evaluated. A time window is used to avoid unwanted reflections and a Hanning window is applied, as a function of the radial distance, to the amplitude of the measured pressure. The real and imaginary parts of the surface impedance of the fibrous material were measured for an angle of incidence varying from 0° up to 81° and for frequencies from 300 Hz up to 6 kHz. The surface impedance as a function of the angle of incidence at 500 Hz, 700 Hz, 1 kHz, and 3 kHz, is presented in Fig. 2.

C. Comparison between predictions and measurements

The main effect of the anisotropy is that the real part of the surface impedance increases with the angle of incidence. This was already noted by Allard *et al.*[6] This effect is observed at 500 Hz, 700 Hz, 1 kHz, and 3 kHz. This is due to the relatively smaller value of ratio σ^{xy}/σ^{z} than one which is the isotropic case. It is more pronounced at medium frequencies of 500 and 700 Hz. The measurements in Fig. 2 are indicated by full circles, the dashed lines represent simulated surface impedances for the isotropic case, and the solid lines are the predicted surface impedances for the anisotropic case. The material data used in the calculation of the impedance of the isotropic material are the parameters measured in the z direction (indicated by the superscript z in Table I). Near normal incidence, the difference between measurement and the calculations, is negligible. With increasing angle of incidence, the difference between the isotropic case and the measured values increases due to the anisotropy. The influence of the anisotropy is most pronounced in the midfrequency range (500–700 Hz). The difference between the surface impedance calculated for the isotropic case, and the surface impedance measured and predicted when the anisotropy is taken into account, decreases with increasing frequency. Even if our model is more general than a transversely isotropic rigid frame model, it should be noticed that for the proposed example, the results are nearly similar thereby reducing the sensitivity to mechanical properties. A decrease in the imaginary part of the surface impedance with the angle of incidence, smaller than the increase in the real part, is predicted at 0.5, 0.7, and 1 kHz. This decrease does not appear in the measurements. This small discrepancy is probably due to a systematic error in the measurements mainly due to the difficulty of keeping constant the height of the microphones.

IV. CONCLUSION

A description of wave propagation in transversely isotropic porous materials was performed in terms of a TMM developed in the context of a recent formulation of the Biot theory. With the new formulation, the expressions of the matrix elements are simplified. As an illustration of the method, the surface impedance of a highly porous material was measured as a function of frequency and of the angle of incidence, and comparisons were performed with predictions obtained with the TMM. It was shown that the anisotropy can have a significant influence on the acoustical behavior of the material. A good agreement was found between theoretical and experimental results.

[1] M. A. Biot, "Theory of propagation of elastic waves in a fluid-filled saturated porous solid," J. Acoust. Soc. Am. **28**, 168–191 (1956).

[2] M. A. Biot, "Mechanics of deformation and acoustic propagation in porous media," J. Appl. Phys. **33**, 1482–1484 (1962).

[3] J. Carcione, "Wave propagation in anisotropic, saturated porous media: Plane-wave theory and numerical simulation," J. Acoust. Soc. Am. **99**, 2655–2666 (1996).

[4] A. K. Vashishth and P. Khurana, "Waves in stratified anisotropic poroelastic media: A transfer matrix approach," J. Sound Vib. **277**, 239–275 (2004).

[5] K. Liu and Y. Liu, "Propagation characteristic of Rayleigh waves in orthotropic fluid-saturated porous media," J. Sound Vib. **271**, 1–13 (2004).

[6] J. F. Allard, R. Bourdier, and A. L'Esperance, "Anisotropy effect in glass wool on normal impedance in oblique incidence," J. Sound Vib. **114**, 233–238 (1987).

[7] K. Attenborough, "Acoustical characteristics of porous materials," Phys. Rep. **82**, 179–177 (1982).

[8] D. Wilson, "Relaxation-matched modeling of propagation through porous media, including fractal pore structure," J. Acoust. Soc. Am. **94**, 1136–1145 (1993).

[9] M. Delany and E. Bazley, "Acoustical properties of fibrous absorbent materials," Appl. Acoust. **3**, 105–116 (1970).

[10] M. Melon, D. Lafarge, B. Castagnede, and N. Brown, "Measurement of tortuosity of anisotropic acoustic materials," J. Appl. Phys. **78**, 4929–4932 (1995).

[11] M. Melon, E. Mariez, C. Ayrault, and S. Sahraoui, "Acoustical and mechanical characterization of anisotropic open-cell foams," J. Acoust. Soc. Am. **104**, 2622–2627 (1988).

[12] V. Tarnow, "Dynamic measurements of the elastic constants of glass wool," J. Acoust. Soc. Am. **118**, 3672–3678 (2005).

[13] D. Johnson, J. Koplik, and R. Dashen, "Theory of dynamic permeability and tortuosity in fluid-saturated porous media," J. Fluid Mech. **176**, 379–403 (1987).

[14] Y. Champoux and J. F. Allard, "Dynamic tortuosity and bulk modulus in air-saturated porous media," J. Appl. Phys. **70**, 1975–1979 (1991).

[15] J. F. Allard, *Propagation of Sound in Porous Media: Modelling Sound Absorbing Materials* (Elsevier Aplied Science, New York, 1993).

[16] O. Dazel, B. Brouard, C. Depollier, and S. Griffith, "A alternative Biot's displacement formulation for porous materials," J. Acoust. Soc. Am. **121**, 3509–3516 (2007).

[17] L. M. Brekhovskikh, *Waves in Layered Media* (Academic, New York, 1960).

[18] C. Depollier, "Theorie de Biot et Prdiction des Proprits Acoustiques des Matriaux Poreux, Propagation dans les milieux Acoustiques Dsordonns (Biot's theory and properties of sound absorbing materials. Propagation in disorders porous materials)," thesis, Universit du Maine, France (1989).

[19] B. Brouard, D. Lafarge, and J. F. Allard, "A general method of modelling the acoustical properties of layered materials including fluid, elastic, and porous layers," in *ICA* (Trondheim, Norway, 1995).

[20] M. Etchessahar, S. Sarhraoui, L. Benyahia, and J. Tassin, "Frequency dependence of the elastic properties of acoustic foams," J. Acoust. Soc. Am. **117**, 1114–1121 (2005).

[21] P. Leclaire, L. Kelders, W. Lauriks, M. Melon, N. Brown, and B. Castagnede, "Determination of the viscous and thermal characteristic lengths by ultrasonic measurements in helium and air," J. Appl. Phys. **80**, 2009–2012 (1996).

[22] M. Tamura, "Spatial Fourier transform method of measuring reflection coefficients at oblique incidence. I Theory and numerical examples," J. Acoust. Soc. Am. **88**, 2259–2264 (1990).

[23] M. Tamura, J. F. Allard, and D. Lafarge, "Spatial Fourier transform method of measuring reflection coefficients at oblique incidence. II Experimental results," J. Acoust. Soc. Am. **97**, 2255–2262 (1995).